

EFFECT OF HOT IONS AT LCLS-II*

L. Wang[#], T. O. Raubenheimer, SLAC, Stanford, CA 94309, USA*Abstract*

The ions in a linac with high repetition rate, such as ERL, draw more attention recently. LCLS-II has a long linac with 1 MHz repetition rate. The ions, in general, are not deeply trapped due to the long bunch spacing. The effect of ion thermal energy becomes important in this regime. The beam dynamics with ions are studied both theoretically and numerically. There is a linear growth in amplitude, instead of exponential growth as traditional fast ion instability. This linear growth set a maximum bunch-train length to limit the beam amplitude to fractional beam sigma. We also extend our works to different regimes where the motions of ions from stable to partially stable.

INTRODUCTION

The new LCLS-II high-repetition rate FEL project at SLAC [1] will use a new superconducting linac composed of TESLA-like RF cavities in continuous wave (CW) operation, in order to accelerate a 1-MHz electron beam to 4 GeV. Figure 1 shows the optics (top) of the hard x-ray beam and the beam size (100 pC) of LCLS-II linac (bottom). The new superconducting linac is driven by a new high-rate injector [2], will replace the existing SLAC copper linac in sectors 1-7 (101.6 m/sector), while the remaining Cu RF structures in sectors 7-10 will be removed and replaced with a simple beam pipe and focusing lattice (the “linac extension”). The existing 2 km PEP-II bypass line (large β section in Fig. 1) will be modified to transport electrons from the linac extension in sector 10 through more than 2.5 km and into either of two undulators in the existing LCLS undulator hall. The overall design of the linac can be found in [3].

There is a low temperature ($\sim 2\text{K}$) for the superconducting linac (L1, L2, L3 in Fig. 1), while the rest linac has room temperature ($\sim 300\text{K}$) with a thermal energy about 0.04eV . In most storage ring light source, the beam potential is much large than 1eV , for instance 100eV for SPEAR3 beam. Therefore, the thermal energy of the ion can be safely neglected. In LCLS-II, the beam is small and the bunch spacing is long where the thermal energy is comparable and even larger than the beam potential. In this case, the thermal energy should be included. The effective ion size with the thermal energy effect can be estimated as

$$\sigma_i^2 \approx \frac{\sigma_e^2}{2} + \frac{v_0^2}{2\omega^2} = \alpha^2 \sigma_e^2, \quad (1)$$

where σ_e is the electron beam size, v_0 is the ion speed at the thermal energy. When the thermal energy is negli-

gible, the ion size is about $1/\sqrt{2}$ times of the electron beam size.

This paper is organized as the following: section II presents the detail simulations and section III introduces our theoretical model to explain the feature of the simulations.

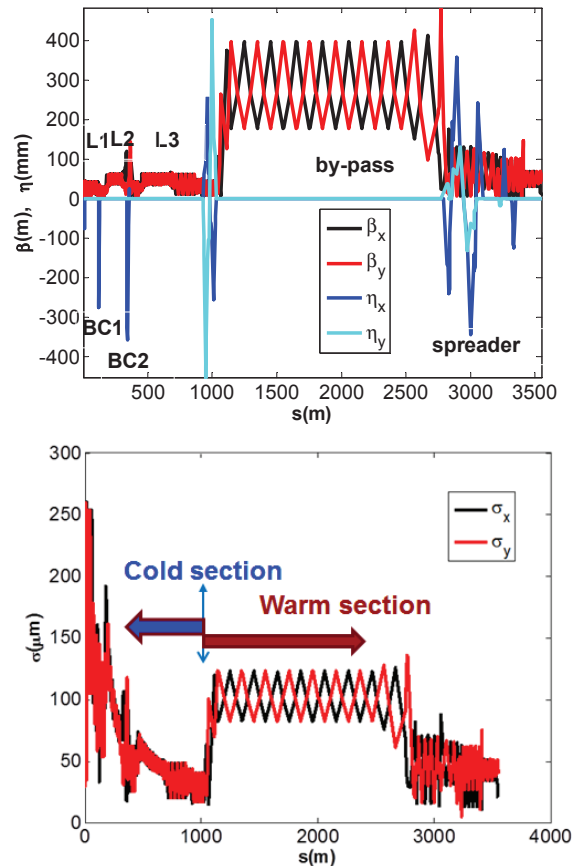


Figure 1: Optics (HXR) (top) and beam size (100 pC, bottom) of the LCLS-II linac.

SIMULATION

Simulations have a number of advantages: the non-linearity of the ion-cloud force is automatically included; the effects of beam optics and bunch-train with arbitrary beam filling pattern can be easily handled; a realistic vacuum model with multi-gas species is straightforward in simulation. A Particle in Cell (PIC) code based on a wake-strong model is used here [4].

The temperature is set to 10 K and 300K in the superconducting linac and warm section, respectively. In simulation we use multiple gases vacuum model [H2 (90%), H2O (1%), CO2 (1%), CO (7%) and CH4 (1%)]. We will use this vacuum component through this paper. The total vacuum pressure of 1 nTorr and 10 nTorr are assumed for the cold and warm section, respectively. The real vacuum should be better.

*Work supported by Department of Energy Contract No. DE-AC02-76SF00515

[#]wanglf@SLAC.stanford.edu

The simulation is done from injector exit (100MeV beam) to the beginning of the undulator. Figure 2 shows the ion distribution along the linac for 100 pC bunch charge. The ions are accumulated mainly at L1, L2 and bypass beam line due to the large beam size there. The motions of ions in other locations are basically unstable due to the over-focusing of the electron beam to the ion particles. Figure 3 shows the *rms* ion size along the linac. It is about twice of the electron beam size at the long-bypass beamline (warm section). The ion beam size estimated from Eq. (1) (using CO ion) is about 3 times of the electron beam size, which is close to the simulation where multiple gas species are used. The transverse distribution of ions at the long by-pass beamline is close to a Gaussian distribution (there is a long tail for far away particles which are excluded) as shown in Fig. 4. This is totally different from the case when the thermal energy is negligible where the ion size is smaller than the electron beam size and there is a sharp peak density at the core part of ion beam [4]. The thermal energy and long bunch spacing makes the dynamics of the beam-ion in LCLS-II totally different from the typical storage ring light sources.

Figure 5 shows the growth of the amplitude of electron bunches along the bunch train at the end of LCLS-II linac. The growth is linear along the bunch train [or time] instead of exponential one in the case of Fast Beam Ion Instability [5]. The linear growth is the result of the linear growth of the ions density along the bunch train. Therefore the amplitude roughly linearly depends on the ion density. Since the electron beam is round, there is a similar growth in both horizontal and vertical planes. The detail oscillation of electron beam and ion beam [Fig. 5 bottom] doesn't show the same oscillation pattern between the two beams, which indicates the lack of coherent motion. One possible reason is that the length of the bunch train is not long enough to allow the instability [coupled motion] start. However simulation with longer bunch train and high vacuum pressure always give linear growth.

Figure 6 shows the case of 300 pC bunch. It basically shows the similar feature as 100 pC, linear growth in time and incoherent motion. The growth is slightly faster than 100 pC case. In short summary, the growth of electron bunch amplitude linearly depends on the ion density. In other words, the amplitude grows linearly with along the bunch train length.

Large beam oscillation amplitude can degrade the performance of LCLS-II FEL. Therefore the ion effect sets a maximum length of the bunch train. For example, tolerable amplitude growth of 1% (10%) beam size limits the bunch train length to 0.5 seconds (15 seconds) and 0.38 seconds (12.5 seconds) for 100 pC and 300 pC bunch charge, respectively. For lower bunch rate than 1 MHz, the tolerable bunch train length should be longer.

A bunch train gap can be used to clear the ions. In general a train gap of a few ion oscillation periods can effectively clear the ions. A simulation shows that a train

gap with 10 missing bunches is good enough to clear more than 95% ions.

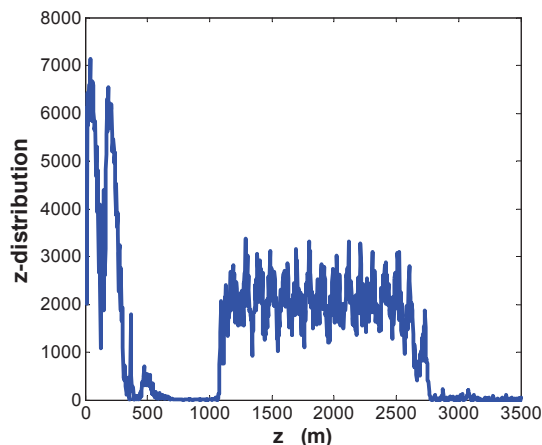


Figure 2: The distribution of ions along the linac, 100 pC bunch.

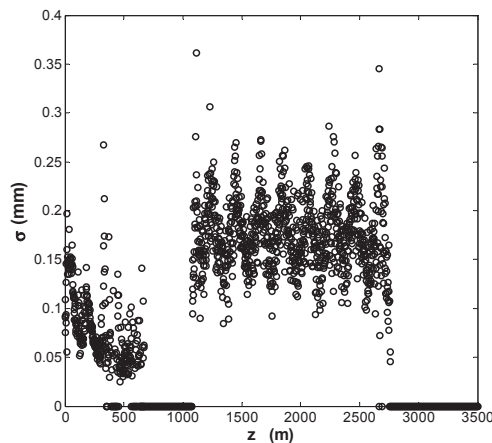


Figure 3: The transverse *rms* size of ions along the linac.

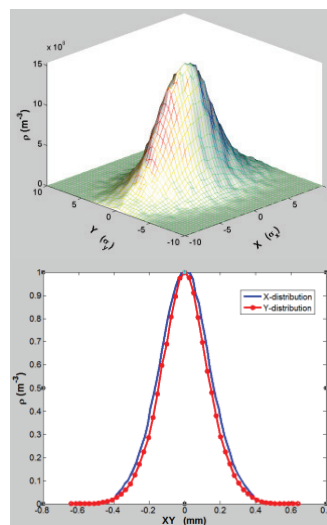


Figure 4: Transverse ion distribution (2D, top) (1D, bottom) at the long bypass beam line for 100 pC bunch charge.

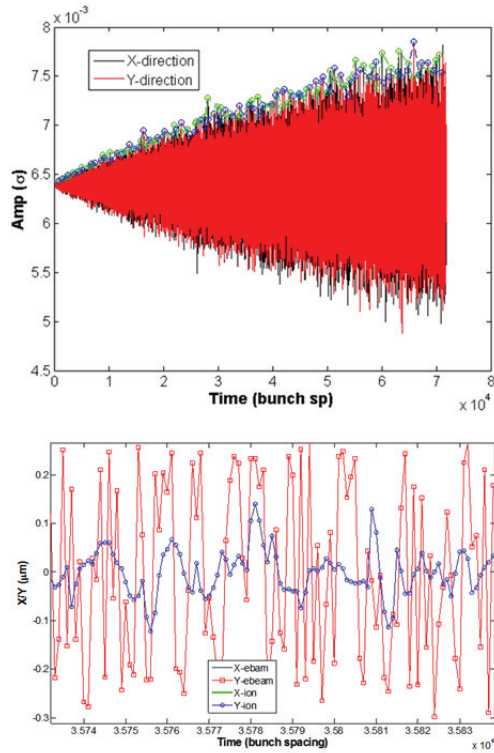


Figure 5: Electron bunch amplitude at the end of linac for a long bunch train (top) and oscillation of electron beam (red line) and ion beam (blue line) (bottom). Bunch charge is 100 pC.

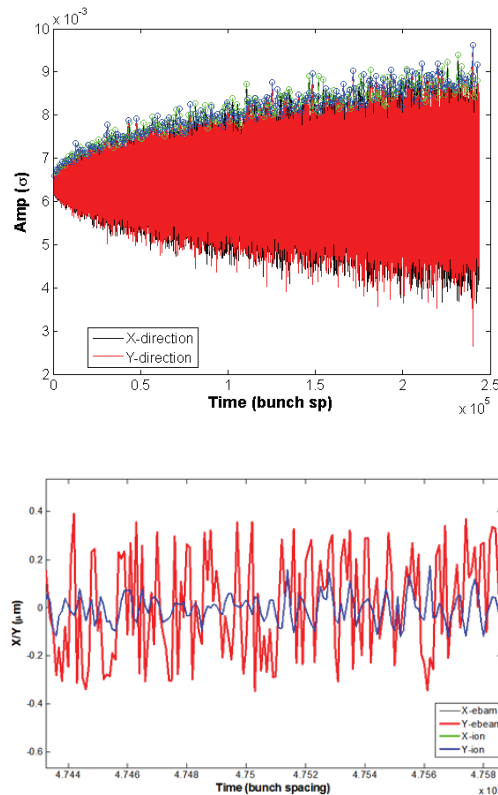


Figure 6: Electron bunch amplitude at the end of linac for a long bunch train (top) and oscillation of electron beam and ion beam (bottom). Bunch charge is 300 pC.

ION FREQUENCY SPREAD OF COLD AND HOT IONS

To understand the simulation, the motion of ions and their frequency spread under different conditions are investigated in this section for both cold and hot ion beams, coasting and bunched electron beam.

Cold ions with Coasting Electron Beam

For a round beam, the potential and field can be written as

$$U(r) = \frac{\lambda_e e}{4\pi\epsilon_0} \left[\gamma - Ei \left(-\frac{r^2}{2\sigma^2} \right) + \ln \left(\frac{r^2}{2\sigma^2} \right) \right] \quad (2)$$

$$E_r(r) = \frac{e\lambda_e}{4\pi\epsilon_0} \frac{1}{r} \left[1 - e^{-\frac{r^2}{2\sigma^2}} \right] \quad (3)$$

where $\gamma=0.57721$ is the Euler gamma constant and Ei is the exponential integral function. λ_e is the bunch line density and σ is the transverse root mean square (*rms*) beam size of the electron bunch. The period of ion oscillation depends on the position of the ion was born r_0 as

$$T(r_0) = 4 \int_0^{r_0} \frac{1}{v(r)} dr = 2\sqrt{2m} \int_0^{r_0} \frac{1}{\sqrt{U(r_0)-U(r)}} dr \quad (4)$$

The energy conservation law is used and the thermal effect is neglected here. Figure 7 shows the calculated ion frequency from the above equation and the results from particle tracking. There is an excellent agreement.

The frequency distribution in general case is given by

$$\rho(\omega_x) = \int_0^\infty \int_0^\infty f(\omega_x, x_0, y_0) g(x_0, y_0) dx_0 dy_0 \quad (5)$$

Here ω_x refers to the horizontal frequency and $f(\omega, x_0, y_0)$ is the frequency distribution function of ions with amplitude of $r_0 = \sqrt{x_0^2 + y_0^2}$. $g(x_0, y_0)$ is the distribution function of ion oscillation amplitude, which varies with time when beam instability happens. When the thermal energy is negligible (strong beam) compared to the beam potential and the electron beam amplitude is smaller compared to its beam size, the distribution of ion oscillation amplitude is a Gaussian distribution with the same *rms* as the electron beam.

Figure 8(a) shows the distribution of ion frequency with a round electron beam when $g(r_0)$ is a Gaussian distribution with *rms* size equal to the electron beam size σ . This is the case of the beginning of the instability where the amplitude is smaller than the beam size.

After instability occurs, the ions oscillate at larger amplitude. The ion frequency spread also increases accordingly. Figure 8(b) and 8(c) show the cases of ion amplitude has a amplitude of $\sqrt{2}\sigma$ and 2σ , respectively. The larger amplitude induces a larger frequency spread and therefore a stronger damping to the instability. The self-damping mechanism is one important character of

beam ion instability, which limits the amplitude of electron beam on orders of beam size at saturation level in most storage ring light sources.

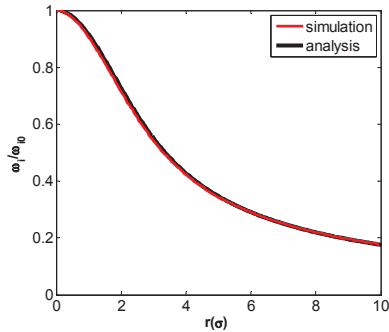


Figure 7: Comparison of the ion frequency with a round electron beam. The analysis is given by Eq. (4).

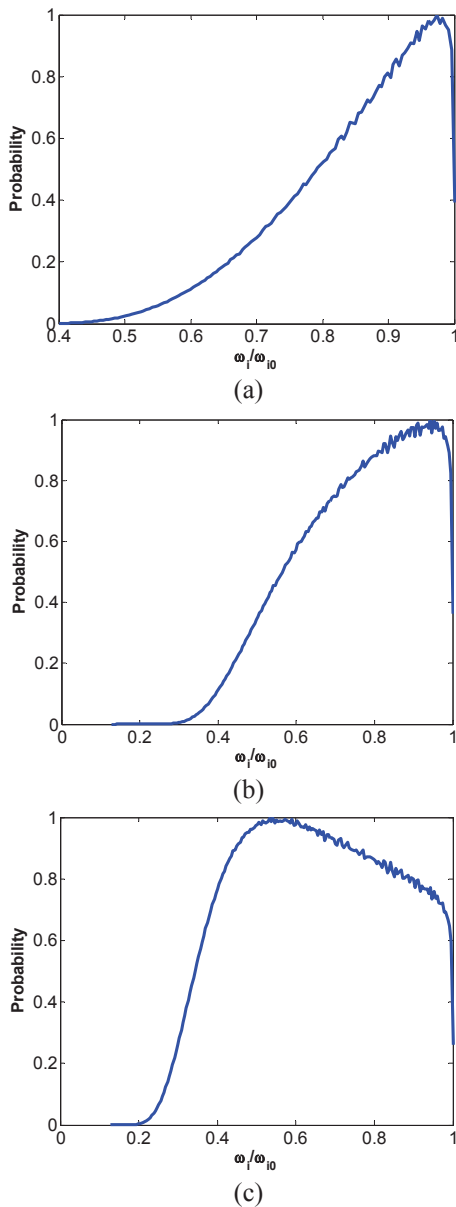


Figure 8: Horizontal ion frequency distribution of a round beam. r_0 has Gaussian distribution with $rms = \sigma$ (a); $\sqrt{2}\sigma$ (b); 2σ (c).

Cold Ions with Bunched Electron Beam

In real accelerators, most electron beams are short bunched beam. When the bunch spacing is much shorter compared to the period of the ion oscillation, as for most storage ring light sources, the electron bunch can be treated as a continuous beam. In this section we investigate the bunch spacing effect on the stable motion of the ions. A particle tracking program is used to estimate the frequency of the ions with different amplitudes.

Figure 9 shows the frequency dependence on the ion amplitude for different bunch spacing $\Delta t = T_0/20, T_0/9, T_0/6.4, T_0/4.5$ and $T_0/3.7$. Here T_0 is the period of the ions near beam centre. The ion frequency with short bunch spacing, such as $\Delta t < T_0/10$, is close to the case with coasting electron beam. When the bunch spacing is long, for example $\Delta t > T_0/9$, the motion of ions with large amplitude becomes unstable (with noisy distribution or zero frequency in the plots). The area of stable motion becomes smaller when the bunch spacing increases. Note that there are some stable/unstable zones for the last three cases. It is a feature of bunched beam. The motion of ion is unstable at smaller amplitude while it can become stable at large amplitude. Here the motion of ions with long bunch spacing is far from sinusoidal oscillations with single frequency. For example, the motion with a period of 5 bunch spacing is unstable; however it becomes stable if the period is 4 bunch spacing. That explains why the ion motion becomes stable at larger amplitude. It is the effect of bunched beam where the ion receives only a few discrete kickers from the electron bunches over one ion oscillation period. If the bunch spacing is longer than $T_0/5$, the motion of the ions is unstable except the core part ($r \sim \sigma$).

Hot Ions with Bunched Electron Beam

In the above studies, the effect of ion temperature is neglected. When the thermal energy of an ion is smaller compared to the beam potential energy ($kT \ll m\omega^2 \sigma^2$), the temperature effect is negligible. This is true for most electron beam in rings where the bunch spacing is short. For instance, the SPEAR3 beam has a bunch spacing of 2 ns and $T_0/\Delta t = 36$. The horizontal frequency at 300K is shown in Fig. 10, which is similar to the result at zero temperature except some noisy feature at large amplitude. It is clear that the effect of temperature is negligible for such strong electron beam.

When bunch spacing is long, the ion drift during one bunch spacing due to the thermal energy can be comparable to the transverse beam size. In LCLS-II, the maximum bunch repetition rate is 1 MHz . The bunch charge varies from 10 pC to 300 pC . For a 100 pC bunch, the CO^+ frequency at the long by-pass beamline is shown in Fig. 11 for zero temperature and 300K, respectively. With zero temperature the bunch spacing effect ($T_0/\Delta t \sim 6$ here) is similar as one shown in Fig. 9. The long bunch spacing makes the ion motion at large amplitude unstable. The effect of temperature at 300K causes the frequency

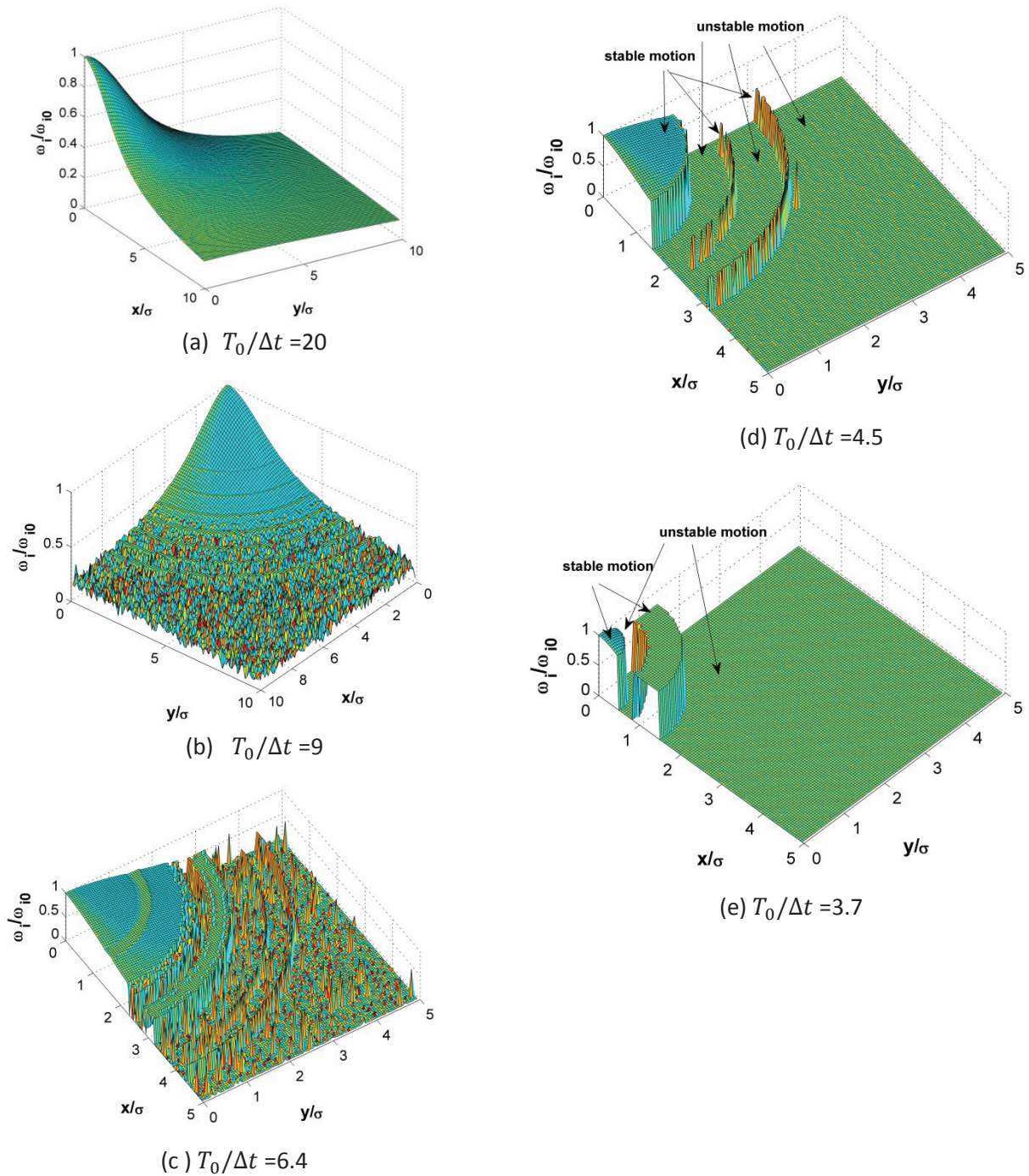


Figure 9: Horizontal Ion frequency distribution of a round beam with various bunch spacing.

distribution more randomly distributed (Fig. 11, bottom). This means that there is weak coherent central motion due to the long bunch spacing. The effect of temperature further suppresses the coherent motion of ions.

BENCHMARK WITH IDEAL LINAC

To better check the effect of temperature and bunch spacing, we set-up one simple numerical test here: a 9 km long linac with regular FODO optics and single gas

species vacuum. There is small variation in ion frequency for FODO cell optics. Therefore we can check the pure effect of bunch spacing and temperature with such ideal linac. The temperature is set to 300K in all cases while the bunch spacing is varied. Figure 12 shows three cases with different bunch spacing of $T_0/\Delta t = 30, 9$ and 5 . There is an exponential growth for both electron and ion beams with a short bunch spacing of $T_0/30$, which is expected by the theory of fast beam ion instability [5]. The electron beam acts to the ions like a coasting beam due to the short

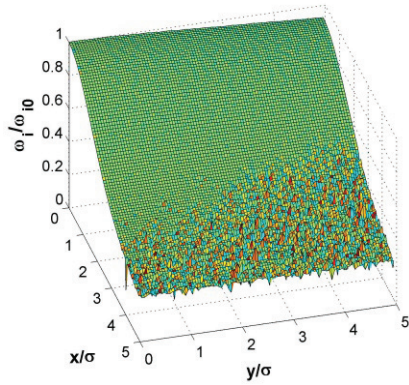


Figure 10: Horizontal ion frequency of a Bi-Gaussian electron beam with $\sigma_x/\sigma_y = 20$ and bunch spacing of 2 ns and Temperature of 300K. $T_0/\Delta t = 36$.

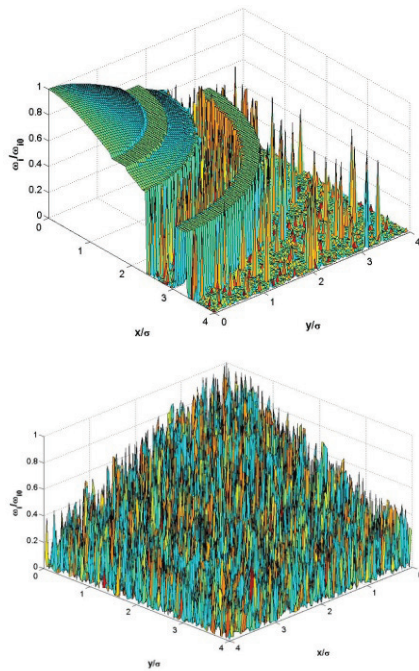


Figure 11: Frequency spread of CO ion at LCLS-II long bypass beamline with $T_0/\Delta t \sim 6$ (100 pC) and bunch repetition rate of 1 MHz at zero temperature (top) and 300K (bottom), respectively.

bunch spacing. When the bunch spacing increases to $T_0/9$, both beams show non-exponential growth with strong beating. The growth becomes linear when the bunch spacing is even longer as $T_0/5$, which is close to the LCLS-II case. Note that ion cloud oscillates at smaller amplitude compared to the electron beam in short bunch spacing case (Fig. 12 top) where the ions are deeply trapped. However the amplitude of ion cloud becomes larger than the electron beam when the bunch spacing is $T_0/5$ long (not shown here) when the ions are not deeply trapped.

The simulation with ideal linac confirms the linear growth in LCLS-II and agrees with the effect frequency spread of hot ions and long bunch spacing.

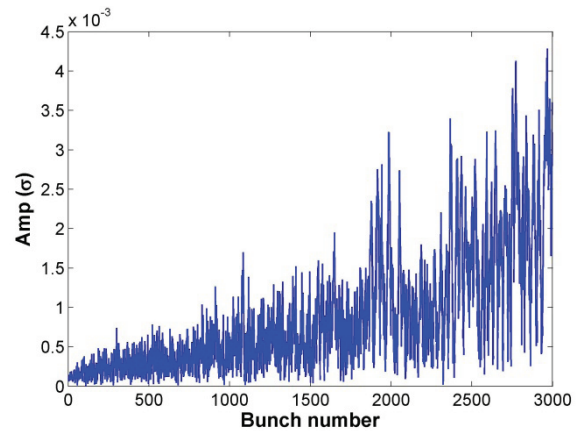
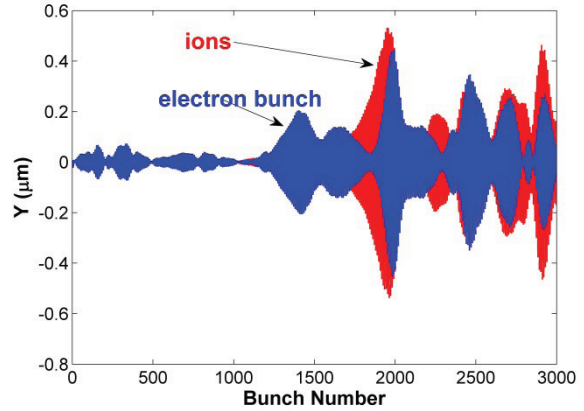
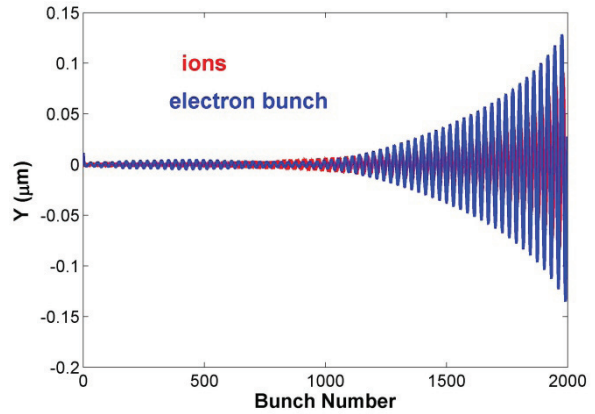


Figure 12: Beam and ion oscillation for various bunch spacing $1/30T_0$ (top), $1/9T_0$ (middle) and $1/5 T_0$ (bottom) in 9 km long FODO cell linac with temperature of 300K. The vertical electron beam size is $15\mu m$.

SUMMARY AND DISCUSSION

A large number of ions can be accumulated due to the attractive force even with long bunch spacing in LCLS-II. However there is a lack of coherent motion between ion and electron beams because of the effects of long bunch spacing and hot ions. As a result, there is a linear growth in amplitude along the bunch train in our case and this growth sets one maximum length of bunch train for the operation. The ions can be effectively cleared by a bunch train gap with length on the order of ion oscillation period.

The frequency spread with hot ions can clearly explain the underlying physics in our case: the long bunch spacing and hot ions together induce large spread and noise in the ion frequency, which causes incoherent ion motion and linear growth of the electron beam.

ACKNOWLEDGEMENTS

We thank our colleagues Gennady Stupakov and William Fawley for fruitful discussions. This work is supported by Department of Energy Contract No. DE-AC02-76SF00515.

REFERENCES

- [1] T. Raubenheimer, “The LCLS-II, a New FEL Facility at SLAC”, in Proc. of 36th Int. Free-Electron Laser Conf., Basel, 2014, WEB001.
- [2] J. Schmerge *et al.*, “The LCLS-II Injector Design”, in Proc. of 36th Int. Free-Electron Laser Conf., Basel, 2014, THP042.
- [3] P. Emma, *et al.*, “Linear Accelerator Design for the LCLS-II FEL Facility”, in Proc. of 36th Int. Free-Electron Laser Conf., Basel, 2014, THP025.
- [4] L. Wang, Y. Cai, T. O. Raubenheimer and H. Fukuma, Phys. Rev. ST Accel. Beams 14, 084401 (2011).
- [5] T. O. Raubenheimer and F. Zimmermann, Phys. Rev. E 52, 5487 (1995).